IEEE Photonics Journal
An IEEE Photonics Society Publication

Effect of Correlation on BER Performance of the FSO-MISO System With Repetition Coding Over Gamma–Gamma Turbulence

Volume 9, Number 5, October 2017

Richa Priyadarshani, *Student Member, IEEE*
Manav R. Bhatnagar, *Senior Member, IEEE*
Zabih Ghassemlooy, *Senior Member, IEEE*
Stanislav Zvanovec, *Member, IEEE*

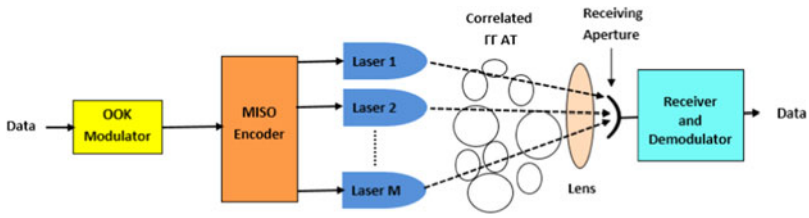

DOI: 10.1109/JPHOT.2017.2738098
1943-0655 © 2017 IEEE

Effect of Correlation on BER Performance of the FSO-MISO System With Repetition Coding Over Gamma–Gamma Turbulence

Richa Priyadarshani,[1] ***Student Member, IEEE*,**
Manav R. Bhatnagar,[1] ***Senior Member, IEEE*,**
Zabih Ghassemlooy,[2] ***Senior Member, IEEE*,**
and Stanislav Zvanovec,[3] ***Member, IEEE***

[1]Department of Electrical Engineering, Indian Institute of Technology Delhi, New Delhi 110016, India
[2]Optical Communications Research Group, School of Computing, Engineering and Information Sciences, Northumbria University, Newcastle upon Tyne, NE1 8ST U.K.
[3]Department of Electromagnetic Field, Czech Technical University in Prague, Prague 16627, Czech Republic

DOI:10.1109/JPHOT.2017.2738098

Manuscript received July 12, 2017; revised August 4, 2017; accepted August 5, 2017. Date of publication August 11, 2017; date of current version September 8, 2017. This work was supported in part by the Science and Engineering Research Board (SERB), Department of Science and Technology, Government of India for the Project "Quantized Feedback Based Collocated and Distributed Wireless Communication Systems: Study and Hardware Implementation" (Project Ref. No. EMR/2016/000592). Corresponding author: Richa Priyadarshani (e-mail: richa.priyadarshani@ee.iitd.ac.in.)

Abstract: In free space optical (FSO) communication systems, atmospheric turbulence is the major cause of bit error rate (BER) performance degradation. The error performance of the system can be significantly improved with the help of spatial diversity by employing multiple transmit or receive apertures. However, correlation of channels under turbulence in the case of small separation between transmit apertures can substantially reduce the benefits of spatial diversity. Still, a thorough analysis of the system performance in terms of diversity order and coding gain for the FSO multiple-input single-output (MISO) system under turbulence influenced correlated channels has not been studied when the repetition coding is used to achieve improved BER performance. In this paper, we provide unique results of the BER performance analysis of the considered correlated FSO-MISO system over Gamma–Gamma distributed turbulence channel. Using the joint moment generating function of received signal-to-noise ratio (SNR), a novel generalized approximate BER expression is derived, followed by convergence test of the power series based BER expression using the Cauchy's ratio test. Then, an asymptotic analysis at high SNR is performed to obtain a novel closed-form expression for BER of FSO-MISO system. We also derive expressions for coding gain, diversity gain, and coding gain loss due to correlation in channels. Although the effect of correlation in channels on the BER performance of the system is analyzed under different scenarios, while it is observed that it does not affect the diversity order; it significantly degrades the coding gain of the considered system.

Index Terms: Diversity, free-space optical (FSO) communications, multivariate gamma-gamma ($\Gamma\Gamma$) distribution, spatial diversity.

1. Introduction

In recent years, free space optical (FSO) communications has emerged as an efficient, and most promising technology for addressing the problems of existing radio frequency communication systems in particular applications. This has been made possible because of the advantages offered by FSO, such as high data rate, high security, large bandwidth, license-free spectrum, easy and quick deployability, and lower power and low mass requirements [1], [2].

However, FSO links face various challenges because of the random behavior of the propagation channel. Atmospheric turbulence (AT), which is the major source of both random intensity and phase fluctuations of received optical signal, degrades the system performance because of signal fading and phase induced distortion (dispersion) [3]. It has already been well established in the literature that the impact of AT can be significantly reduced by means of spatial diversity using multiple apertures at the transmitter (Tx), and/or at the receiver (Rx) [4]–[6]. In [7] and [8], it has been reported that the repetition coding (RC) outperforms the orthogonal space-time block code (OSTBC) in intensity modulation/direct detection (IM/DD) FSO systems with on-off keying (OOK), and subcarrier intensity modulated multiple-input-single-output. In RC system, a copy of the information signal is transmitted from all the transmit apertures simultaneously.

Many statistical turbulence models are available which describe the behavior of the irradiance fluctuations in FSO for single optical links. For Gamma-Gamma ($\Gamma\Gamma$) turbulence model, it has been shown that there is an excellent agreement between the theoretical and experimental data for various AT regimes (weak, strong, and saturation) [2], [9], [10]. For uncorrelated FSO channels, the transmit apertures must be separated by the spatial coherence distance, which exceeds the fading correlation length [2], [11]. However, in many cases the available space at the transmitting head may not be sufficient to attain such requirement, practically. For such scenarios, however, there is still missing a thorough description of correlated channels, which is the most typical case practically experienced. Therefore, in this paper we analyse an OOK IM/DD FSO link with a correlated $\Gamma\Gamma$ AT channel. We assume a FSO multiple-input-single-output (MISO) system, where the transmit lasers are closely and equally spaced to ensure constant correlation of particular channels influenced by AT [9], [12]. An example of practical realization of this model is the use of three transmit lasers at the vertices of an equilateral triangle. Similarly, for four transmit lasers, constant correlation can be achieved approximately by placing them on the vertices of a square (considering the size of Tx is significantly small)[1]. On the other hand, a two transmit lasers-based system is a very special case. In this set-up, RC is adopted as the spatial diversity technique.

The outage performance of selection combining Rx over a constant correlated $\Gamma\Gamma$ AT link was studied in [9]. In [13] and [14] the performance analysis of diversity systems over $\Gamma\Gamma$ AT channel was investigated. However, in [14] $\Gamma\Gamma$ random variables (RVs) were considered to be independent. An exponentially correlated fading channel model was used to investigate the outage probability of the selection combining Rx, and the bit error rate (BER) performance of the maximal ratio combining Rx in [13]. However, the analysis of these previous results are mostly based on the outage probability, which does not give clear insights of the impact of correlation on the BER performance of the FSO system. For practical implementation of a FSO system, it is very important to have a clear understanding of the impact of correlation on the link BER performance. To the best of the author's knowledge, no works on the analysis of the impact of correlation on the BER performance of the FSO-MISO system with RC has been reported in the literature yet.

Motivated by aforesaid discussions, we make the following specific contributions in this paper.

1) An approximated analytical expression for the joint moment generating function (MGF) of *M* correlated squared and weighted $\Gamma\Gamma$ RVs in the form of power series is derived.
2) A novel approximate BER expression for RC over correlated $\Gamma\Gamma$ fading in the form of power series is derived. A convergence test using the Cauchy's ratio test is performed to show that the series converges for a finite number of summations.

[1]such that the difference between the length of diagonal, and edge of the square is of the order of wavelength of the carrier frequency.

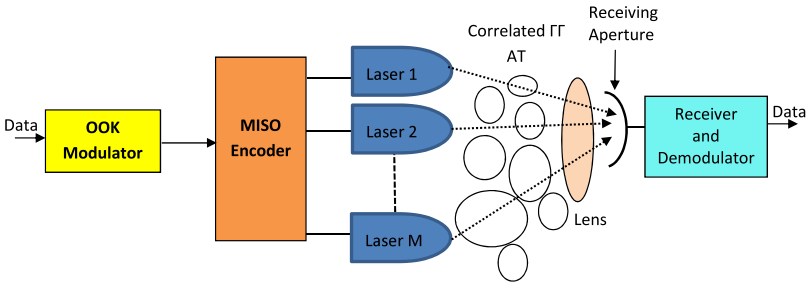

Fig. 1. Block diagram of FSO-MISO system.

3) Asymptotic BER analysis at higher signal-to-noise ratio (SNR) is also performed to gain insights of the impact of correlation on both the diversity and coding gains of the system under different scenarios. Expressions for the diversity gain, coding gain, and coding gain loss are also derived using the asymptotic BER analysis.
4) The effect of variation of correlation on the BER performance is analysed under medium to strong AT. And furthermore, for a fixed value of correlation level the BER performance analysis is carried out for range of AT regimes.
5) To shed lights on the asymptotic properties of the considered system in the presence of correlation in AT channel, we provide important observations on the diversity order and coding gain of the system based on the obtained BER plots.

The rest of the paper is organized as follows.

System and channel models are introduced in Section 2. In Section 3, an approximated joint MGF of the received SNRs over correlated $\Gamma\Gamma$ AT is derived. Using the derived approximated MGF expression, an approximated BER expression for the FSO-MISO system with RC is derived. Further, asymptotic BER analysis at higher SNR is also carried out to obtain the expression for diversity order, coding gain, and coding gain loss, in Section 4. Numerical results are presented and discussed in Section 5. Finally Section 6 provides useful conclusions based on the numerical results and the observations given.

2. System and Channel Models

In this section, we will present the system and channel model of the considered FSO-MISO system; followed by derivation of expression for the joint pdf of the received SNRs.

2.1 System Model

Let us consider an IM/DD FSO-MISO system consisting of M transmit lasers, and a single receiving aperture at the receiver as shown in Fig. 1. The information bit stream is converted into a non-return to zero OOK format with RC, and simultaneously used for IM of multiple laser sources for transmission over a correlated $\Gamma\Gamma$ AT channel [15]. Using a single receiving aperture-based receiver makes the need of any combining method unnecessary, thus resulting in a simpler receiver.

The signal received at the Rx is given by:

$$r = \sqrt{E_b} s \sum_{i=1}^{M} h_i + n, \tag{1}$$

where $E_b = \frac{\eta^2 I^2}{M}$, η represents optical-to-electrical conversion coefficient, I is the light intensity received at the detector through a clear air channel with no AT, h_i is the correlated channel statistically defined by $\Gamma\Gamma$ RV, s is the transmitted symbol $s \in \{0,1\}$, and n represents the additive white Gaus-

sian noise (AWGN) at the detector input with zero mean and variance of $N_0/2$. A maximum-likelihood (ML) detection scheme is employed at the detector with the help of the estimated symbol $\tilde{s}$:

$$\hat{s} = \min_{\tilde{s}\in\{0,1\}} \left| r - \sqrt{E_b}\tilde{s}\sum_{i=1}^{M} h_i \right|^2. \tag{2}$$

2.2 Channel Model

Here, we use $\Gamma\Gamma$ turbulence model to describe the fading behavior of a FSO channel. Let I_i denotes the received signal irradiance of the link between the ith transmit aperture and the receive aperture due to the AT, and it can be represented by [11], [16]:

$$I_i = I h_i, \tag{3}$$

where h_i is the correlated $\Gamma\Gamma$ RV. Here we assume that, the degradation of optical signal is mainly because of AT, therefore we do not include the path loss difference, since in the case of close transmit apertures it is minimal. Note from (3) that, I_i is also correlated with the $\Gamma\Gamma$ distribution. The joint probability distribution function (pdf), i.e., $f_{I_1,\ldots,I_M}(I_1, \ldots, I_M)$ of M $\Gamma\Gamma$ RVs I_i involving effect of correlation between channels is given as [9], [13]:

$$f_{I_1,\ldots,I_M}(I_1, \ldots, I_M) = \frac{2^M(1-\sqrt{\rho})^\alpha}{\Gamma(\alpha)\Gamma(\beta)^M} \sum_{k_1,\ldots,k_M=0}^{\infty} \Gamma(\alpha + k_1 + \ldots + k_M) \frac{\rho^{\frac{k_1+\ldots+k_M}{2}}}{(1+(M-1)\sqrt{\rho})^{\alpha+k_1+\ldots+k_M}}$$
$$\times \left(\frac{\alpha\beta}{\Omega(1-\sqrt{\rho})}\right)^{\frac{M\alpha+k_1+\ldots+k_M+M\beta}{2}} \prod_{i=1}^{M} \frac{1}{\Gamma(\alpha+k_i)k_i!} I_i^{\frac{\alpha+k_i+\beta}{2}-1} K_{\alpha+k_i-\beta}\left(2\sqrt{\frac{\alpha\beta I_i}{\Omega(1-\sqrt{\rho})}}\right), \tag{4}$$

where $K_v(\cdot)$ is the modified Bessel function of the second kind of order v [17], $0 \le \rho < 1$ denotes the correlation coefficient, $\Omega = E[I_i^2]$, α and β are the AT parameters, the expectation $E[I_i] = 1$, and the variance $Var[I_i] = \sigma^2 = \frac{1}{\alpha} + \frac{1}{\beta} + \frac{1}{\alpha\beta}$. Note that, the AT parameters depend on Rytov variance σ_R^2, which represents irradiance fluctuations associated with the AT [18], [19].

By using Jacobian technique for the transformation of RVs, the joint pdf of the received SNRs of M diversity branches can be obtained as [20, Ch. 6]:

$$f_{\gamma_1,\ldots\gamma_M}(\gamma_1, \ldots\gamma_M) = |J| f_{I_1,\ldots,I_M}(I_1, \ldots, I_M)\Big|_{I_i=\sqrt{\frac{\gamma_i}{\mu_i}}}, \tag{5}$$

where $|J|$ represents the determinant of the jacobian matrix, γ_i and μ_i represent instantaneous and average received SNRs, respectively.

Substituting (4) in (5), and using transformation of the Bessel function into Meijer-G function [21, Eq. (8.4.23.1)], and employing the symmetry and translation properties of Meijer-G function [21, Eq. (8.2.2.15)], we obtain the joint pdf of the received SNRs as:

$$f_{\gamma_1,\ldots.\gamma_M}(\gamma_1, \ldots.\gamma_M) = \frac{(1-\sqrt{\rho})^\alpha}{\Gamma(\alpha)\Gamma(\beta)^M} \sum_{k_1\ldots k_M=0}^{\infty} \left[\Gamma(\alpha + k_1 + \ldots k_M)\right.$$
$$\left. \times \frac{\rho^{\frac{k_1+\ldots+k_M}{2}}}{(1+(M-1)\sqrt{\rho})^{\alpha+k_1+\ldots+k_M}} \prod_{i=1}^{M} \frac{1}{\Gamma(\alpha+k_i)(k_i)!2^M} (\sqrt{\gamma_i})^{-2} G_{0,2}^{2,0}\left(\Xi\sqrt{\frac{\gamma_i}{\mu_i}}\,\middle|\, \begin{matrix} \cdot,\cdot \\ \alpha+k_i,\ \beta \end{matrix}\right)\right], \tag{6}$$

where $G_{p,q}^{m,n}(\cdot|\cdot)$ is the Meijer-G function[22, Eq. (9.301)] and $\Xi = \alpha\beta/(1-\sqrt{\rho})$.

3. MISO System Performance Evaluation

In this section, we will perform BER analysis of the considered MISO system with RC. For the analysis, we will first derive the joint MGF expression of the received SNRs over correlated $\Gamma\Gamma$ fading. This expression will be further used to derive the BER equation of RC for correlated $\Gamma\Gamma$ AT.

3.1 Joint MGF of the Received SNRs Over Correlated $\Gamma\Gamma$ AT

The expression for joint MGF of the received SNRs (function of squared $\Gamma\Gamma$ RVs) over correlated $\Gamma\Gamma$ AT can be obtained by using (6):

$$\psi_{\gamma_1,\ldots.\gamma_M}(s) = E_{\gamma_1,\ldots\gamma_M}\left[\exp\left(-s\sum_{i=1}^{M}\gamma_i\right)\right], \tag{7}$$

where $E[\cdot]$ denotes the expectation.

Let us represent the exponential term of (7) in terms of Meijer-G function [23, Eq. (11)], and by using [21, Eq. (2.24.1.1)], we have:

$$\psi_{\gamma_1,\ldots.\gamma_M}(s) = \frac{(1-\sqrt{\rho})^{\alpha}}{\Gamma(\alpha)\Gamma(\beta)^M}\sum_{k_1\ldots k_M=0}^{\infty}\left[\Gamma(\alpha+k_1+\ldots k_M)\frac{\rho^{\frac{k_1+\ldots+k_M}{2}}}{(1+(M-1)\sqrt{\rho})^{\alpha+k_1+\ldots+k_M}2^M}\right.$$
$$\left.\times\prod_{i=1}^{M}\left[\frac{1}{\Gamma(\alpha+k_i)(k_i)!}\frac{2^{\alpha+k_i+\beta}}{2\pi}G_{1,4}^{4,1}\left(\left(\frac{\Xi}{\sqrt{\mu_i}}\right)^2\times\frac{1}{16s}\middle|\begin{matrix}1\\ \frac{\alpha+k_i}{2},\frac{\alpha+k_i+1}{2},\frac{\beta}{2},\frac{\beta+1}{2}\end{matrix}\right)\right]\right]. \tag{8}$$

3.2 BER of RC Over Correlated $\Gamma\Gamma$ AT

For the input-output (I/O) relation given by (1), the instantaneous SNR at the Rx for RC is given by [7], [11]:

$$\gamma_{\text{MISO}} = \frac{E_b}{2N_0}\left(\sum_{i=1}^{M}h_i\right)^2, \tag{9}$$

where E_b is the average electrical energy of the transmitted symbol, and h_i is the correlated $\Gamma\Gamma$ RV. Following the similar approach used in [11], the BER of RC over correlated $\Gamma\Gamma$ AT can be written as:

$$P_e = \frac{1}{\pi}\int_0^{\frac{\pi}{2}}E_{\gamma_1,\ldots\gamma_M}\left[\exp\left(-\frac{\left(\sum_{i=1}^{M}\sqrt{\gamma_i}\right)^2}{4M^2\sin^2\theta}\right)\right]d\theta. \tag{10}$$

Assuming that the propagation distance is such that, the condition of variance[2] $\sigma_R^2 < 1$ (excluding saturation regime) is met, we can approximate $(\sum_{i=1}^{M}\sqrt{\gamma_i})^2$ to $M\sum_{i=1}^{M}\gamma_i$ in (10), and use (7) to get the BER expression in terms of MGF [11]:

$$P_e \approx \frac{1}{\pi}\int_0^{\frac{\pi}{2}}\psi\left(\frac{1}{4M\sin^2\theta}\right)d\theta. \tag{11}$$

[2]When turbulence channel is near the ground, and propagation distance of plane wave is approximately few hundred meters, $\sigma_R > 0.5$ denotes a strong AT, and $\sigma_R < 0.1$ represents weak AT [24].

TABLE 1
Value of N for Every k_i for Particular M in (12) for Convergence of Series to Achieve Accuracy at 5th Significant Digit for $\alpha = 2$ and $\beta = 1.4$

ρ	$M = 2$	$M = 3$	$M = 4$
0.2	25	18	12
0.6	30	24	18
0.8	40	42	42

Employing (8) in (11), the BER of the considered system is obtained in the form of:

$$P_e \approx \frac{1}{\pi}\frac{(1-\sqrt{\rho})^{\alpha}}{\Gamma(\alpha)\Gamma(\beta)^M}\sum_{k_1\ldots k_M=0}^{\infty}\left[\Gamma(\alpha+k_1+\ldots+k_M)\frac{\rho^{\frac{k_1+\ldots+k_M}{2}}}{(1+(M-1)\sqrt{\rho})^{\alpha+k_1+..+k_M}2^M}\right.$$
$$\left.\times\int_0^{\frac{\pi}{2}}\prod_{i=1}^{M}\left[\frac{1}{\Gamma(\alpha+k_i)(k_i)!}\frac{2^{\alpha+k_i+\beta}}{2\pi}G_{1,4}^{4,1}\left(\left(\frac{\Xi}{\sqrt{\mu_i}}\right)^2\frac{4M\ \sin^2\theta}{16}\middle|\begin{matrix}1\\ \frac{\alpha+k_i}{2},\frac{\alpha+k_i+1}{2},\frac{\beta}{2},\frac{\beta+1}{2}\end{matrix}\right)\right]d\theta\right]. \quad (12)$$

Let us make some remarks on the derived expression for the BER of the considered system.

1) Because of the complex nature of the integration involved in (12), we use the numerical integration technique to further solve the equation to obtain the results for BER plots.
2) Although the derived expression is for correlated $\Gamma\Gamma$ channel, by setting $\rho = 0$ we obtain the BER expression for RC over uncorrelated $\Gamma\Gamma$ AT. Note that, for $\rho = 0$ only the terms corresponding to $k_1 = k_2 = \cdots = k_M = 0$ contribute to the BER analysis.
3) It can be seen from (12) that the derived BER expression is in the power series form; however, it converges for a finite number of summations (N) as illustrated in Table 1. The Cauchy ratio test [17], [25] is used to prove the convergence of the series of (12), as is given in the next subsection.

Based on the above made remarks, the BER expression for M $\Gamma\Gamma$ distributed uncorrelated FSO links will be:

$$P_e^{(0)} = \frac{1}{2^M\pi\Gamma(\beta)^M}\int_0^{\frac{\pi}{2}}\prod_{i=1}^{M}\left[\frac{1}{\Gamma(\alpha)}\frac{2^{\alpha+\beta}}{2\pi}G_{1,4}^{4,1}\left(\left(\frac{\alpha\beta}{\sqrt{\mu_i}}\right)^2\frac{4M\ \sin^2\theta}{16}\middle|\begin{matrix}1\\ \frac{\alpha}{2},\frac{\alpha+1}{2},\frac{\beta}{2},\frac{\beta+1}{2}\end{matrix}\right)\right]d\theta. \quad (13)$$

3.3 Convergence Test

For the convergence test, we first find Nth and $(N+1)$th terms of the series in (12) as:

$$a_N \approx \frac{1}{\pi}\frac{(1-\sqrt{\rho})^{\alpha}}{\Gamma(\alpha)\Gamma(\beta)^M}\Gamma(\alpha+N+k_2+\ldots+k_M)\frac{\rho^{\frac{N+k_2+\ldots+k_M}{2}}}{(1+(M-1)\sqrt{\rho})^{\alpha+N+k_2+\ldots+k_M}2^M}\frac{2^{(\alpha+N+\beta)}}{\Gamma(\alpha+N)N!}$$
$$\times\frac{1}{2\pi}\int_0^{\frac{\pi}{2}}G_{1,4}^{4,1}\left(\left(\frac{\Xi}{\sqrt{\mu_i}}\right)^2\frac{4M\ \sin^2\theta}{16}\middle|\begin{matrix}1\\ \mathbf{w}'\end{matrix}\right)\prod_{i=2}^{M}\left[\frac{2^{\alpha+k_i+\beta}}{\Gamma(\alpha+k_i)(k_i)!2\pi}G_{1,4}^{4,1}\left(\left(\frac{\Xi}{\sqrt{\mu_i}}\right)^2\frac{4M\ \sin^2\theta}{16}\middle|\begin{matrix}1\\ \mathbf{w}_i\end{matrix}\right)\right]d\theta, \quad (14)$$

where $\mathbf{w}_i = (\frac{\alpha+k_i}{2}, \frac{\alpha+k_i+1}{2}, \frac{\beta}{2}, \frac{\beta+1}{2})$ and $\mathbf{w}' = (\frac{\alpha+N}{2}, \frac{\alpha+N+1}{2}, \frac{\beta}{2}, \frac{\beta+1}{2})$.

$$a_{N+1} \approx \frac{1}{\pi}\frac{(1-\sqrt{\rho})^{\alpha}}{\Gamma(\alpha)\Gamma(\beta)^{M}}\Bigg[\Gamma(\alpha+N+1+k_2+\ldots+k_M)\frac{\rho^{\frac{N+1+k_2+\ldots+k_M}{2}}}{(1+(M-1)\sqrt{\rho})^{\alpha+N+1+k_2+\ldots+k_M}2^{M}}$$
$$\times\frac{2^{(\alpha+N+1+\beta)}}{\Gamma(\alpha+N+1)(N+1)!}\frac{1}{2\pi}\int_0^{\frac{\pi}{2}} G_{1,4}^{4,1}\left(\left(\frac{\Xi}{\sqrt{\mu_i}}\right)^2\frac{4M\ \sin^2\theta}{16}\middle|\begin{matrix}1\\ \mathbf{w}''\end{matrix}\right)$$
$$\times\prod_{i=2}^{M}\left[\frac{1}{\Gamma(\alpha+k_i)(k_i)!}\frac{2^{\alpha+k_i+\beta}}{2\pi}G_{1,4}^{4,1}\left(\left(\frac{\Xi}{\sqrt{\mu_i}}\right)^2\frac{4M\ \sin^2\theta}{16}\middle|\begin{matrix}1\\ \mathbf{w}_i\end{matrix}\right)\right]d\theta\Bigg], \tag{15}$$

where $\mathbf{w}'' = (\frac{\alpha+N+1}{2}, \frac{\alpha+N+2}{2}, \frac{\beta}{2}, \frac{\beta+1}{2})$.

Then, we determine the ratio of (14) and (15) and use the identity $\Gamma(z) = \frac{\Gamma(z+1)}{z}$ to obtain:

$$\frac{a_{N+1}}{a_N} = \frac{(\alpha+N+k_2+\ldots+k_M)\rho^{\frac{1}{2}}}{(1+(M-1)\sqrt{\rho})(\alpha+N)}\frac{2}{(N+1)}$$
$$\times\frac{\int_0^{\frac{\pi}{2}} G_{1,4}^{4,1}\left(\left(\frac{\Xi}{\sqrt{\mu_i}}\right)^2\frac{4M\ \sin^2\theta}{16}\middle|\begin{matrix}1\\ \mathbf{w}''\end{matrix}\right)\prod_{i=2}^{M}\left[G_{1,4}^{4,1}\left(\left(\frac{\Xi}{\sqrt{\mu_i}}\right)^2\frac{4M\ \sin^2\theta}{16}\middle|\begin{matrix}1\\ \mathbf{w}_i\end{matrix}\right)\right]d\theta}{\int_0^{\frac{\pi}{2}} G_{1,4}^{4,1}\left(\left(\frac{\Xi}{\sqrt{\mu_i}}\right)^2\frac{4M\ \sin^2\theta}{16}\middle|\begin{matrix}1\\ \mathbf{w}'\end{matrix}\right)\prod_{i=2}^{M}\left[G_{1,4}^{4,1}\left(\left(\frac{\Xi}{\sqrt{\mu_i}}\right)^2\frac{4M\ \sin^2\theta}{16}\middle|\begin{matrix}1\\ \mathbf{w}_i\end{matrix}\right)\right]d\theta}, \tag{16}$$

where $a_1 = (\alpha + k_2 + \ldots + k_M)$.

All the terms other than the terms with N can be amalgamated to a constant K to obtain:

$$\left|\frac{a_{N+1}}{a_N}\right| = \left|K\frac{(N+a_1)}{(N+\alpha)(N+1)}\right|, \tag{17}$$

where $K =$

$$\frac{2\sqrt{\rho}}{(1+(M-1)\sqrt{\rho})}\frac{\int_0^{\frac{\pi}{2}}\left[G_{1,4}^{4,1}\left(\left(\frac{\Xi}{\sqrt{\mu_i}}\right)^2\frac{4M\ \sin^2\theta}{16}\middle|\begin{matrix}1\\ \mathbf{w}''\end{matrix}\right)\prod_{i=2}^{M}\left[G_{1,4}^{4,1}\left(\left(\frac{\Xi}{\sqrt{\mu_i}}\right)^2\frac{4M\ \sin^2\theta}{16}\middle|\begin{matrix}1\\ \mathbf{w}_i\end{matrix}\right)\right]\right]d\theta}{\int_0^{\frac{\pi}{2}}\left[G_{1,4}^{4,1}\left(\left(\frac{\Xi}{\sqrt{\mu_i}}\right)^2\frac{4M\ \sin^2\theta}{16}\middle|\begin{matrix}1\\ \mathbf{w}'\end{matrix}\right)\prod_{i=2}^{M}\left[G_{1,4}^{4,1}\left(\left(\frac{\Xi}{\sqrt{\mu_i}}\right)^2\frac{4M\ \sin^2\theta}{16}\middle|\begin{matrix}1\\ \mathbf{w}_i\end{matrix}\right)\right]\right]d\theta}. \tag{18}$$

By applying Cauchy's ratio test [17, ch. 5], [25, ch. 10] on (17), we get:

$$\lim_{N\to\infty}\left|\frac{a_{N+1}}{a_N}\right| \to 0. \tag{19}$$

For a set of N for different values of ρ as given in Table, (12) converges. Hence, it is proved that the series converges. It should also be noted that, K remains constant with respect to any variation of N.

Observation 1: It can be observed from Table 1, that higher values of N are required for higher correlation coefficients. However, the increase in the number of transmitting lasers does not always raise the number of terms N required for the summation.

4. Asymptotic BER Analysis

It is not possible to get any insights of the diversity order and the coding gain of the system from (12). Therefore, for a better understanding of the system's performance, the asymptotic BER analysis at higher SNR is performed in this section.

4.1 Diversity Gain and Coding Gain

At higher SNR, the coding gain G_c and diversity gain G_d are the two parameters that are used to analyze the BER performance. For asymptotic analysis at higher SNR, we replace Meijer-G function in (12) by the generalized hypergeometric function (using Slater's theorem [21]), and consider the terms corresponding to $k_i = 0$ to obtain the asymptotic BER:

$$\tilde{P}_e \approx \frac{1}{\pi}\frac{(1-\sqrt{\rho})^{\alpha}}{\Gamma(\alpha)\Gamma(\beta)^M}\frac{\Gamma(\alpha)}{\left(1+(M-1)\sqrt{\rho}\right)^{\alpha}2^M}\int_0^{\frac{\pi}{2}}\prod_{i=1}^{M}\left[\frac{2^{\alpha+\beta}}{\Gamma(\alpha)2\pi}\sum_{h=1}^{4}\prod_{j=1}^{4}\Gamma(b_j-b_h)^*\Gamma(b_h)\right.$$
$$\left.\times Z^{b_h}{}_1F_3\left((-1)^{-4}Z\,\middle|\,\begin{matrix} b_h \\ \left[1+b_h-\mathbf{b_q}\right]^*\end{matrix}\right)\right]d\theta, \tag{20}$$

where $Z = \left(\frac{\Xi}{\sqrt{\mu_i}}\right)^2\frac{4M\,\sin^2\theta}{16}$. Moreover, the asterisk sign signifies that for $j = h$, we ignore the contribution of the Gamma function in the product terms by replacing $\Gamma(0)$ with 1, and in the argument of hypergeometric function, the vector $\left[1+b_h-\mathbf{b_q}\right]^* = \left[(1+b_h-b_1),...,(1+b_h-b_j),..,(1+b_h-b_q)\right]$ will have only $(q-1)$ terms as the term with index $j = h$ can be ignored (where $q = 4$). At higher SNR, the hypergeometric function in (20) can be approximated to unity [17, Ch. 5], [26] and the integral term is simplified with only a trigonometric term. After some rearrangements, and simplification of (20), we obtain:

$$\tilde{P}_e \approx \frac{1}{\pi}\frac{(1-\sqrt{\rho})^{\alpha}}{\Gamma(\alpha)\Gamma(\beta)^M}\frac{\Gamma(\alpha)}{\left(1+(M-1)\sqrt{\rho}\right)^{\alpha}2^M}\int_0^{\frac{\pi}{2}}\left[\prod_{i=1}^{M}\left[\frac{2^{\alpha+\beta}}{\Gamma(\alpha)2\pi}\sum_{h=1}^{4}\Gamma(b_h)\Gamma(b_1-b_h)^*\right.\right.$$
$$\left.\left.\times\,\Gamma(b_2-b_h)^*\Gamma(b_3-b_h)^*\Gamma(b_4-b_h)^*\left(\frac{\Xi}{\sqrt{\mu_i}}\right)^{2b_h}\left(\frac{M}{4}\sin^2\theta\right)^{b_h}\right]d\theta\right], \tag{21}$$

where $b_1 = \frac{\alpha}{2}$, $b_2 = \frac{\alpha+1}{2}$, $b_3 = \frac{\beta}{2}$ and $b_4 = \frac{\beta+1}{2}$.

At higher SNR, the term with the smallest exponent of average SNR μ_i in (21) dominates the BER [4]. Note that, the exponent of average SNR $\mu_i = b_h$, which has four terms; and following solving the minimization problem, the diversity gain of the system is obtained as:

$$G_d = M\,\min\left\{\frac{\alpha}{2},\frac{\beta}{2}\right\}, \tag{22}$$

where $\min\{\cdot,\cdot\}$ represents the minimum of the two. It should be noted that, if $\alpha < \beta$, then $G_d = \frac{M\alpha}{2}$, else $G_d = \frac{M\beta}{2}$.

To find G_c, and the asymptotic BER we consider only the dominant term of the series in (21) to obtain:

$$\tilde{P_e} \approx A \prod_{i=1}^{M} \left[\frac{2^{\alpha+\beta}}{\Gamma(\alpha)2\pi} \Gamma(G_d/M) \Gamma\left(b_1 - \frac{G_d}{M}\right)^* \Gamma\left(b_2 - \frac{G_d}{M}\right)^* \Gamma\left(b_3 - \frac{G_d}{M}\right)^* \Gamma\left(b_4 - \frac{G_d}{M}\right)^* \times (\Xi)^{\frac{2G_d}{M}} \right] \left[\int_0^{\frac{\pi}{2}} \left(\frac{M}{4}\sin^2\theta\right)^{G_d} d\theta \right] \mu^{-G_d}, \tag{23}$$

where $A = \dfrac{1}{\pi} \dfrac{(1-\sqrt{\rho})^{\alpha}\Gamma(\alpha)}{\Gamma(\alpha)\Gamma(\beta)^M \left(1+(M-1)\sqrt{\rho}\right)^{\alpha} \times 2^M}$.

Using [22, Eq.(3.62.3)], (23) can be further simplified to the following form:

$$\tilde{P_e} \approx A \prod_{i=1}^{M} \left[\frac{2^{\alpha+\beta}}{\Gamma(\alpha)2\pi} \Gamma(G_d/M) \Gamma\left(b_1 - \frac{G_d}{M}\right)^* \Gamma\left(b_2 - \frac{G_d}{M}\right)^* \Gamma\left(b_3 - \frac{G_d}{M}\right)^* \Gamma\left(b_4 - \frac{G_d}{M}\right)^* \times (\Xi)^{\frac{2G_d}{M}} \left(\frac{M}{4}\right)^{\frac{G_d}{M}} \frac{(2\frac{G_d}{M}-1)!!}{(\frac{2G_d}{M})!!} \frac{\pi}{2} \right] \mu^{-G_d}, \tag{24}$$

where $(\cdot)!!$ represents double factorial.

It is well established in the literature that the asymptotic BER at higher SNR is given by [4]:

$$\tilde{P_e} \approx (G_c \mu)^{-G_d}. \tag{25}$$

From (24) and (25), G_c of the system is given by:

$$G_c = \left(A \prod_{i=1}^{M} \left[\frac{2^{\alpha+\beta}}{\Gamma(\alpha)2\pi} \Gamma(G_d/M) \Gamma\left(b_1 - \frac{G_d}{M}\right)^* \Gamma\left(b_2 - \frac{G_d}{M}\right)^* \Gamma\left(b_3 - \frac{G_d}{M}\right)^* \Gamma\left(b_4 - \frac{G_d}{M}\right)^* \times (\Xi)^{\frac{2G_d}{M}} \left(\frac{M}{4}\right)^{\frac{G_d}{M}} \frac{(2\frac{G_d}{M}-1)!!}{(\frac{2G_d}{M})!!} \frac{\pi}{2} \right] \right)^{-1/G_d}. \tag{26}$$

4.2 Coding Gain Loss Due to Correlation

The coding gain loss ΔG_c^L can be calculated by taking the logarithmic of the ratio of G_c at a fixed value of ρ to the value of G_c at non-correlated ρ as follow:

$$\Delta G_c^L = 10 \log_{10} \left(\frac{G_c^{(\rho)}}{G_c^{(0)}} \right). \tag{27}$$

Using the values of G_c from Table 2 for 2, 3, and 4 transmit lasers in (26), the coding gain loss at different correlation levels can be determined as illustrated in Table 3.

Observation 2: The diversity order of the considered system depends only on α, β, and M, while, it does not depend on ρ as can be seen from (22).

Observation 3: G_c of the system depends on α, β, M, as well as ρ. For clear understanding of dependence of G_c on correlation, we replace all the terms other than the terms having ρ with a constant K in (26) to get $G_c = \left[\frac{(1-\sqrt{\rho})^{\alpha-2G_d}}{(1+(M-1)\sqrt{\rho})^{\alpha}} \right]^{-1/G_d} K^{-1/G_d}$. It can be clearly seen that G_c decreases with the increasing value of ρ. Reduction in G_c when changing from correlated towards non-correlated ρ is more significant when the number of transmit lasers exceeds two.

TABLE 2
Value of G_c (dB) for Different Values of Correlation Coefficient at Fixed Values of $\alpha = 2$ and $\beta = 1.4$

ρ	$M = 2$	$M = 3$	$M = 4$
0	0.02876	0.0184	0.01709
0.2	0.02872	0.01825	0.01
0.6	0.02785	0.00946	0.006
0.8	0.01982	0.00465	0.0024
0.95	0.0093	0.0011	0.0004
0.99	0.00374	0.000204	0.00005

TABLE 3
Coding Gain Loss $\Delta\ G_c^L$ (dB) for Different Correlation Levels at Fixed Values of $\alpha = 2$ and $\beta = 1.4$

ρ	$M = 2$	$M = 3$	$M = 4$
0.2	0.006	0.035	0.64
0.6	0.01	2.87	4.5
0.8	1.6	6.0	8.5
0.95	5.0	12.2	16.3
0.99	8.9	19.5	25.3

5. Numerical Results and Discussion

In this section, we provide a detailed discussion upon the effect of AT channels correlation on the BER performance of the considered MISO system under different scenarios. Analytical plots, obtained by using the derived results of Section 3, are validated by Monte Carlo simulations. The power series based expression in (12) is truncated to a finite number of terms N, to obtain the analytical BER results. For generating correlated $\Gamma\Gamma$ RVs in MATLAB, the algorithm proposed in [27] is used.

Fig. 2 shows the BER plot of the FSO-MISO system with two transmit apertures and $\Gamma\Gamma$ AT. It is assumed that the transmit lasers send the same copies of the signal in parallel over a correlated channel for AT parameters of $\alpha = 2$, and $\beta = 1.4$. It is also assumed that, both receive diversity branches have almost the same average SNR. The BER versus SNR plots are obtained for correlation levels $\rho = 0$, 0.2, 0.6, and 0.8. The corresponding simulated BER plots are also shown in the figure. As can be seen from the figure that there is a close match between the simulated and analytical BER plots for all considered values of SNR; this confirms the validity of the proposed analysis. By observing the relative shift of BER versus SNR plots along x-axis in Fig. 2, it can be determined that the performance of the considered system degrades in terms of the coding gain by approximately 2 dB at $\rho = 0.6$ as compared to $\rho = 0.2$ at a BER of 10^{-4}.

In Fig. 3, the BER performance against the SNR is plotted for the FSO-MISO system with two transmit lasers, different values of AT parameters, and $\rho = 0.2$. It can be observed from the figure that the system performs better under moderate AT ($\alpha = 4, \beta = 1.9$) as compared to strong AT ($\alpha = 2, \beta = 1.4$), both in terms of the diversity order and the coding gain. Under moderate AT, a

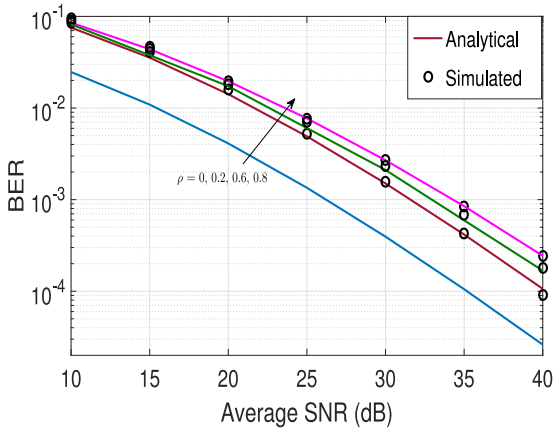

Fig. 2. Comparison of analytical and simulated BER versus average SNR plots for two transmit lasers-based FSO-MISO system for $\alpha = 2$ and $\beta = 1.4$ with various values of ρ.

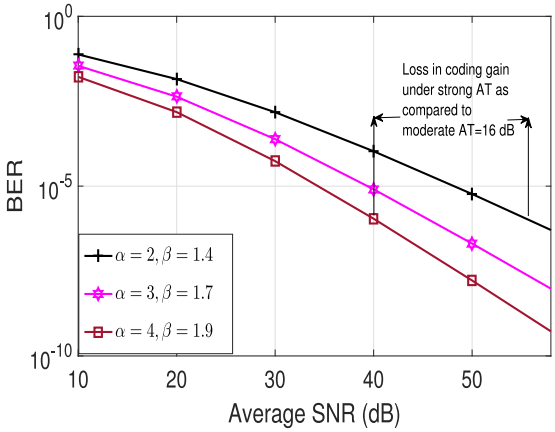

Fig. 3. Analytical BER plots for 2 transmit lasers system for different turbulence parameters α and β and a fixed value of $\rho = 0.2$.

diversity order of 1.9 is achieved as compared to the diversity order of 1.4 under strong AT. At a BER of 10^{-3}, the SNR penalty is 16 dB under strong AT compared to moderate AT. It can also be observed that diversity order of $\min\{\alpha, \beta\}$ is achieved in this case as the number of transmit lasers is two. It is in agreement with the derived expression of diversity gain (22).

Figs. 4 and 5 illustrate the asymptotic BER versus the average SNR for FSO-MISO system with 2 and 3 Txs and different values of ρ of channels obtained under strong AT with $\alpha = 2$, $\beta = 1.4$. In Fig. 4, we compare the BER plots obtained from asymptotic analysis of Section 4 with the predicted results of Section 3 for 2 and 3 Txs showing a close match for different correlation levels at higher SNR, thus validating our asymptotic analysis. Fig. 5 shows that at a BER of 10^{-5} the 2 Txs-based system offers the SNR penalty of approximately 5 dB for $\rho = 0.95$ compared to uncorrelated fading, i.e., $\rho = 0$. However, for the system with 3 Txs, the SNR penalty increases up to 12.23 dB for a very high correlation level, i.e., $\rho = 0.95$, as compared to the uncorrelated fading scenario. For the values of AT parameters being considered, G_d for 2 Txs and 3 Txs-based system are β and $\frac{3\beta}{2}$, respectively, as per our derivation (22). From Fig. 5, we calculate the diversity order by taking the logarithm of the BER values obtained at SNR values of 70 dB and 60 dB for different values of ρ. From Fig. 5, for 2 Txs-based system, we obtain a BER of 1.16×10^{-7} at a SNR of 70 dB and a BER of 2.8×10^{-6} at a SNR of 60 dB for $\rho = 0.95$. This leads to the diversity order of $1.38 \approx \beta = 1.4$.

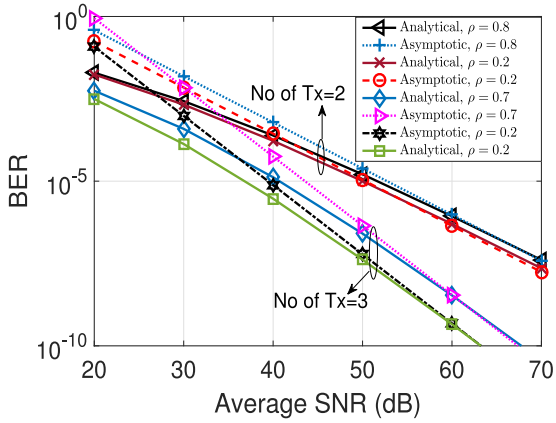

Fig. 4. Analytical and asymptotic BER plots for the FSO-MISO system with 2, 3 Txs, $\rho = 0.2, 0.7$, and 0.8., and $\alpha = 2$, $\beta = 1.4$.

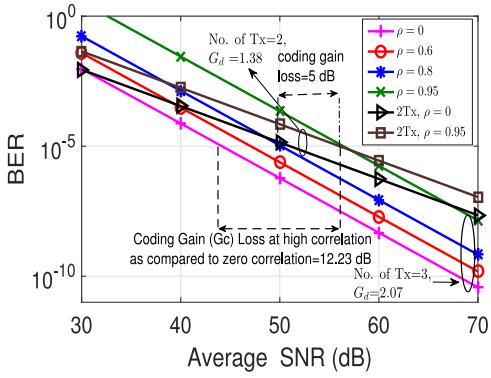

Fig. 5. Coding gain loss at high correlation as compared to uncorrelated case for 2 and 3 transmit lasers at $\alpha = 2$, $\beta = 1.4$.

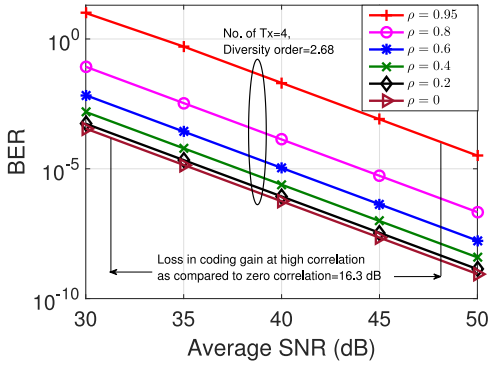

Fig. 6. Coding gain loss at high correlation as compared to uncorrelated case for 4 transmit lasers at $\alpha = 2$, $\beta = 1.4$.

While, for the 3 Txs-based system, the diversity order of 2.07 $\approx \frac{3\beta}{2} = 2.1$ is obtained. The diversity order for other values of ρ determined from Fig. 5 proved to be independent of correlation between channels.

In Fig. 6, the number of transmitting lasers is increased to four. At a BER of 10^{-4} a SNR penalty of 16.3 dB is observed at $\rho = 0.95$ as compared to the uncorrelated scenario. Following the similar procedure adopted for 2 and 3 Txs, the diversity order in this case is calculated to be 2.68 $\approx$ 2.7 $\approx 2G_d$. Here also it is observed that the diversity order is independent of ρ.

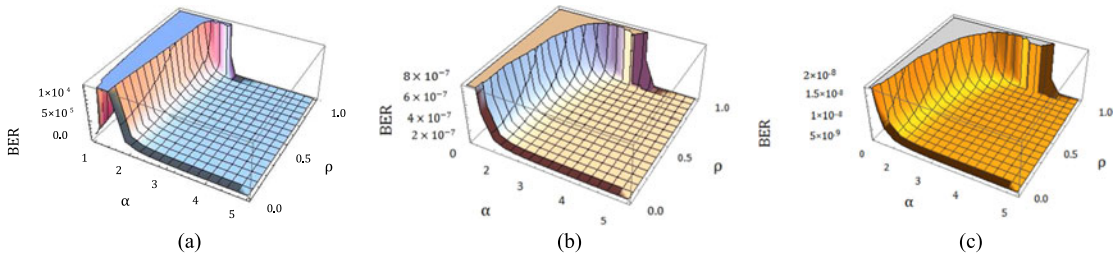

Fig. 7. BER versus α versus ρ plots for different cases at a SNR = 50 dB. (a) Plot for 2 transmit lasers at $\beta = 1.4$. (b) Plot for 3 transmit lasers at $\beta = 1.4$. (c) Plot for 4 transmit lasers at $\beta = 1.2$.

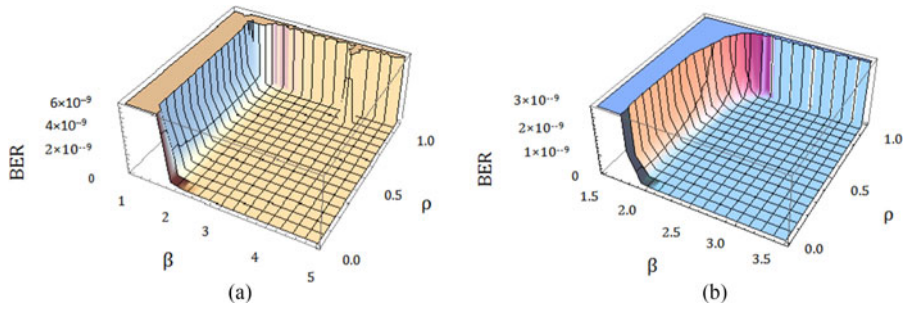

Fig. 8. BER versus β versus ρ plots for different cases at $\alpha = 3$. (a) Plot for 2 transmit lasers at a SNR = 60 dB. (b) Plot for 3 transmit lasers at a SNR = 40 dB.

Table 3 summarizes the results obtained from the asymptotic analysis, carried out to observe the SNR penalty for different values of ρ for the considered system under different scenarios at $\alpha = 2$, $\beta = 1.4$. It is observed that for the system with only 2 Txs, the SNR penalty is low when ρ is increased from 0.2 to 0.6. But, as we increase ρ from 0.6 to 0.95, there is a relatively higher SNR penalty of approximately 5 dB. When the system is almost fully correlated, i.e., $\rho = 0.99$, there is a SNR penalty of approximately 8.9 dB as compared to uncorrelated system. However, for the FSO-MISO system with 3 and 4 Txs, even small change in ρ causes a significant change in the SNR requirement. For 3 Txs-based system, the SNR penalty is 19.5 dB at $\rho = 0.99$, which is high compared to the uncorrelated system. While, for 4 Txs-based system, the SNR penalty is approximately 25 dB at $\rho = 0.99$, which is very high.

Fig. 7 shows the BER versus α versus ρ plot for the system with two, three, and four transmit lasers. The 3D plot is obtained at an average SNR of 50 dB. From Fig. 7(a), it can be observed that for $1 < \alpha < 1.5$, the maximum value of BER of 10^{-4} (which is below the FEC limit of 3.8×10^{-3}) incurs at a moderate value of $\rho < 0.6$. However, at $\alpha = 2$, the maximum value of BER is observed only when transmit apertures become approximately fully correlated, i.e., $\rho \geq 0.9$. It can also be observed that irrespective of the correlation level, the BER is approximately zero for $3 < \alpha < 5$. Note that, the system performance becomes worst when the maximum value of BER is incurred. In Fig. 7(b), the number of transmit lasers is increased from two to three. Improvement in the BER performance is observed as its maximum value is reduced to 8×10^{-7} as compared to the two lasers-based system. However, because of increase in the number of Txs, the BER performance degrades much more rapidly due to correlation among channels. In Fig. 7(c), the number of Txs is further increased to four. The BER performance is further improved as its maximum value is reduced to 2×10^{-8} as compared to the three lasers-based system. However, because of increase in the number of transmit lasers, degradation in the BER performance due to correlation becomes much significant. The maximum value of BER incurs when the system becomes fully correlated even under weak AT.

Fig. 8 shows the BER versus β versus ρ plot for the system with two and three transmit lasers for $\alpha = 3$, and average SNR values of 60 dB and 40 dB. It can be observed from Fig. 8(a),

that the BER performance is poor for $1 < \beta < 2$, irrespective of the correlation level. For $2 < \beta < 5$, the BER performance degrades only at a very high correlation level of $\rho > 0.8$; this effect is prominent at $\beta = 4$. In Fig. 8(b), the number of transmit lasers is increased from two to three; and it can be observed from the figure that this system gives better performance even at worse SNR value of 40 dB as compared to the SNR of 60 dB of the previous case with 2 Txs. However, performance degradation at very high correlation level (when $\rho \to 1$) is observed in this case as well.

6. Conclusion

We have derived a novel BER expression for the FSO-MISO system for repetition coding over correlated $\Gamma\Gamma$ fading link. The derived series based expression of BER was shown to converge for a finite value of summation in dependence on correlation and number of diversity branches within studied FSO model. It was shown analytically that change in the correlation coefficient did not cause any alteration in the diversity order of the system but it substantially degraded the SNR requirement of the system. The proposed analysis shed substantial light over asymptotic behaviour of the considered system. We also derived expressions for diversity order, coding gain, and coding gain loss of the system. With the help of proposed analysis, it was shown that for the system with more than two transmit lasers, very small change in the correlation level can substantially degrade the BER performance of the system. However, for the FSO system with only two transmit lasers, impairment in the BER performance was observed only when the correlation level changed from low value of 0.2 to very high value of 0.8. Further, we also studied the BER performance under different AT regimes, and was shown analytically that under moderate AT we achieved a significant performance gain both in terms of the diversity order and the coding gain as compared to the strong AT. 3D plots were also obtained to observe the BER performance by varying any two parameters from α, β, and ρ, at a time for the considered system with two, three, and four transmit apertures.

References

[1] H. Kaushal and G. Kaddoum, "Optical communication in space: Challenges and mitigation techniques," *IEEE Commun. Surveys Tut.*, vol. 19, no. 1, pp. 57–96, Jan.–Mar. 2016.

[2] Z. Ghassemlooy, W. Popoola, and S. Rajbhandari, *Optical Wireless Communications: System and Channel Modelling With MATLAB*. Boca Raton, FL, USA, CRC Press, 2012.

[3] M. Uysal, C. Capsoni, Z. Ghassemlooy, A. Boucouvalas, and E. Udvary, *Optical Wireless Communications-An Emerging Technology*. New York, NY, USA: Springer, 2016.

[4] M. R. Bhatnagar and Z. Ghassemlooy, "Performance evaluation of FSO MIMO links in gamma-gamma fading with pointing errors," in *Proc. 2015 IEEE Int. Conf. Commun*, Jun. 2015, pp. 5084–5090.

[5] M. R. Bhatnagar and S. Anees, "On the performance of Alamouti scheme in gamma-gamma fading FSO links with pointing errors," *IEEE Wireless Commun. Lett.*, vol. 4, no. 1, pp. 94–97, Feb. 2015.

[6] M. R. Bhatnagar and Z. Ghassemlooy, "Performance analysis of gamma-gamma fading FSO MIMO links with pointing errors," *J. Lightw. Technol*, vol. 34, no. 9, pp. 2158–2169, May 2016.

[7] M. Safari and M. Uysal, "Do we really need OSTBCs for free-space optical communication with direct detection?" *IEEE Trans. Wireless Commun.*, vol. 7, no. 11, pp. 4445–4448, Nov. 2008.

[8] X. Song and J. Cheng, "Subcarrier intensity modulated MIMO optical communications in atmospheric turbulence," *IEEE J. Opt. Commun. Netw.*, vol. 5, no. 9, pp. 1001–1009, Sep. 2013.

[9] G. T. Djordjevic, M. I. Petkovic, J. A. Anastasov, P. N. Ivanis, and Z. M. Marjanovic, "On the effects of correlation on outage performance of FSO-unbalanced multibranch SC receiver," *IEEE Photon. Technol. Lett.*, vol. 28, no. 12, pp. 1348–1351, Jun. 2016.

[10] M. R. Bhatnagar, "Average BER analysis of differential modulation in DF cooperative communication system over gamma-gamma fading FSO links," *IEEE Commun. Lett.*, vol. 16, no. 8, pp. 1228–1231, Aug. 2012.

[11] M. Abaza, R. Mesleh, A. Mansour, and E. H. M. Aggoune, "Spatial diversity for FSO communication systems over atmospheric turbulence channels," in *Proc. IEEE Wireless Commun. Netw. Conf.*, Apr. 2014, pp. 382–387.

[12] J. Reig, "Multivariate Nakagami-*m* distribution with constant correlation model," *AEU-Int. J. Electron. Commun.*, vol. 63, no. 1, pp. 46–51, Jan. 2009.

[13] K. P. Peppas, G. C. Alexandropoulos, C. K. Datsikas, and F. I. Lazarakis, "Multivariate gamma-gamma distribution with exponential correlation and its applications in radio frequency and optical wireless communications," *IET Microw. Antennas Propag.*, vol. 5, no. 3, pp. 364–371, Feb. 2011.

[14] N. D. Chatzidiamantis and G. K. Karagiannidis, "On the distribution of the sum of gamma-gamma variates and applications in RF and optical wireless communications," *IEEE Trans. Commun.*, vol. 59, no. 5, pp. 1298–1308, May 2011.

[15] M. R. Bhatnagar, "A one bit feedback based beamforming scheme for FSO MISO system over gamma-gamma fading," *IEEE Trans. Commun.*, vol. 63, no. 4, pp. 1306–1318, Apr. 2015.
[16] S. M. Navidpour, M. Uysal, and M. Kavehrad, "BER performance of free-space optical transmission with spatial diversity," *IEEE Trans. Wireless Commun.*, vol. 6, no. 8, pp. 2813–2819, Aug. 2007.
[17] G. Arfken, *Mathematical Methods for Physicists*, 3rd ed., Orlando, FL, USA: Academic, 1985.
[18] G. Yang, M. A. Khalighi, S. Bourennane, and Z. Ghassemlooy, "Fading correlation and analytical performance evaluation of the space-diversity free-space optical communications system," *J. Opt.*, vol. 16, no. 3, 2014, Art. no. 035403.
[19] M. R. Bhatnagar, Z. Ghassemlooy, S. Zvanovec, M. A. Khalighi, and M. M. Abadi, "Quantized feedback-based differential signaling for free-space optical communication system," *IEEE Trans. Commun.*, vol. 64, no. 12, pp. 5176–5188, Dec. 2016.
[20] A. Papoulis and S. U. Pillai, *Probability, Random Variables and Stochastic Processes*, 4th ed., Boston, MA, USA: McGraw-Hill, 2002.
[21] A. P. Prudnikov, Yu Brychkov, and O. I. Marichev, *Integral and Series, Part 3: More Special Functions*, vol. 3, G. G. Gould, Ed. Moscow, Russia: Nauka Publishers, 1990.
[22] I. S. Gradshteyn and I. M. Ryzhik, *Table of Integrals, Series, and Products*, 7th ed., A. Jeffrey, Ed. New York, NY, USA: Academic, 2007.
[23] V. S. Adamchik and O. I. Marichev, "The algorithm for calculating integrals of hypergeometric type functions and its realization in reduce system," in *Proc. Int. Symp. Symbolic Algebr. Comput.*, 1990, pp. 212–224.
[24] X. Zhu and J. M. Kahn, "Markov chain model in maximum-likelihood sequence detection for free-space optical communication through atmospheric turbulence channels," *IEEE Trans. Commun.*, vol. 51, no. 3, pp. 509–516, Mar. 2003.
[25] T. J. I. Bromwich, *Introduction to the Theory of Infinite Series*, 3rd ed. New York, NY, USA: Chelsea, 1991.
[26] Oct. 2001. Available: http://functions.wolfram.com/07.23.03.0001.01, Accessed on: Jul. 2017.
[27] J. Reig, M. A. Martinez-Amoraga, and L. Rubio, "Generation of bivariate Nakagami-*m* fading envelopes with arbitrary not necessary identical fading parameters," *Wireless Commun. Mobile Comput.*, vol. 7, no. 4, pp. 531–537, Sep. 2007.